Proceedings of the Canadian Society for Mechanical Engineering International Congress
Computational Fluid Dynamics Canada International Congress
CSME - CFD-SC2023
May 28-31, 2023, Sherbrooke, QC, Canada

A Comparison of Directional Performance of Articulated Heavy Vehicles

Qinghui Zhou[1], Haonan Zhang[1], Yongzhu Huang[2], Yuping He[3*]
[1]School of Mechanical-Electrical and Vehicle Engineering, Beijing University of Civil Engineering and Architecture, Beijing, China
[2]Beijing Huanda Automobile Assembly Co., Ltd., Beijing, China
[3]Department of Automotive and Mechatronics Engineering, University of Ontario Institute of Technology, Oshawa, Canada
*Yuping.He@uoit.ca

Abstract—With the increase of international logistics supply chains, modular articulated heavy vehicle (AHV) configurations in freight transport are expected to develop rapidly in China. It is in the process to make a decision on Chinese modular AHV configurations, i.e., what modular configuration for AHVs should be firstly developed and deployed? In order to address the issue, two configurations of AHV were evaluated considering the actual transport situations in China. The lateral stability and the maneuverability of the two configurations AHV, i.e., type-A and -B, were examined using multi-body dynamic modelling and simulation. Numerical simulations were conducted to assess the main directional performance measures, i.e., rearward amplification (RWA) and path-following off-tracking (PFOT). Simulations show that the RWA measure of type-B is greater than that of type-A in high-speed evasive maneuvers. In contrast, low-speed PFOT of type-A is larger than that of type-B. Type-A is recommended to be developed first due to the following facts: 1) this AHV exhibits better high-speed lateral stability, 2) the low-speed PFOT of this AHV can be enhanced using advanced vehicle safety systems, e.g., active trailer steering. The achieved results may provide useful guidelines for manufacturers to select and develop effective modular configurations for AHVs.

Keywords-articulated heavy vehicles; high-speed lateral stability; low-speed path-following off-tracking; numerical simulation

I. INTRODUCTION

It is well known that tractor-trailer combinations are a popular means of long-haul freight transportation [1,2]. Among the modular configurations widely used in some countries and regions, double-trailer combinations have a good ability to enhance transportation capacity and reduce carbon emission [3,4]. Compared with traditional tractor/semi-trailer combinations, the transport capacity of double-trailer AHVs can be increased by 50%, greatly improving the transport efficiency. Meanwhile, it can reduce fuel consumption by 10%, decrease transportation cost by 34%, and drop carbon dioxide emissions per ton kilometer [5]. In order to achieve dual carbon goals, i.e., carbon dioxide emission peaking before 2030 and carbon neutrality before 2060, recently, longer combination vehicles (LCVs) are drawn attention, and attempts are being made to discuss their potential applications in China's transportation industry. For example, the China government's policy on sustainable development of transportation promotes the transition of the transport sector towards low-carbon development [6]. Modular transportation, i.e., the application of standardized logistics turnover boxes shall be encouraged, multimodal transport of bult goods can also be promoted, and the mode of drop-and-pull transport may also be emphasized.

However, due to LCVs' longer overall length and heavier weight than tractor/semi-trailer combinations, the stability and the maneuverability of these large vehicles needs to be fully considered and comprehensively explored. An LCV with poor lateral stability generally experiences a higher RWA measure in high-speed single lane-change maneuver. On the other hand, an LCV with poor low-speed PFOT shows a large swept path of trailers, thereby reducing its intersection pass ability. Thus, the last two decades have witnessed numerous studies on improving the safety of LCVs [7]. In AHV designs, there is a trade-off between the lateral stability and the maneuverability, i.e., the former can be improved at the cost of the latter, and vice versa. This trade-off makes the AHV design a challenging task. With the rapid development of highway networks in China, it is crucial to identify effective configurations of LCV with acceptable directional performance.

Many studies have been carried out on the modular configurates of LCVs [8,9]. However, in China, the geometric features of highway ramps and interchanges were mainly designed and built for conventional tractor/semi-trailer combinations, adequate attention has not been paid to the operations of LCVs. Considering the distinguished features of the highway and road networks in China, the modular configurations of LCVs used in Europe and North America may be tailored. Among Europe modular systems (EMS), the longest semi-trailer is 13.6 m, and the overall vehicle combination length can be up to 25.25 m [5]. These vehicle combinations can be constructed in number of ways, as shown in Figure 1.

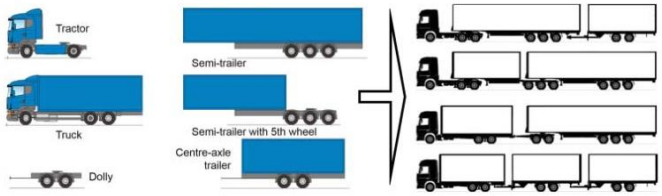

Figure 1. Different configurations in Europe modular system.

In China, the operational scenarios for modular system include intercity highway and urban road logistics, in which the goods delivery is featured with low density and high volume van freight. Therefore, as shown in Figure 2, two LCV configurations may be suitable for these operational scenarios: 1) truck + dolly + semi-trailer (Type-A), and 2) tractor + semi-trailer + center axle trailer (Type-B). In reality, a truck (or tractor + semi-trailer) may be used for goods delivery in urban areas and even travel on city streets; moreover, a truck (or tractor + semi-trailer) can be easily coupled with a trailer to form a LCV to improve fuel economy and transportation efficiency for highway freight transportation. Hence, this research selects these two LCVs to be studied.

(a) Type A: truck + dolly + semi-trailer

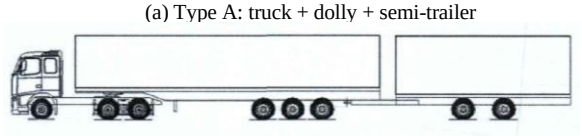

(b) Type B: tractor + semi-trailer + center axle trailer

Figure 2. Configurations of the selected LCVs.

In order to compare the directional performance of the two LCVs, it is necessary to generate the respective models for representing the lateral dynamics of these vehicles. To this end, the lateral stability and the maneuverability are both evaluated and analyzed using multi-body dynamic modelling and simulation using Matlab software. The performance measures, i.e., low-speed PFOT and high-speed RWA, are derived from the specified testing maneuvers. Based on the evaluation of the two LCVs' directional performance, a recommendation was made for manufacturers to select and develop the suitable LCV.

II. VEHICLE SYSTEM MODELS

A. Dynamic model

As shown in Figure 2, each of the two LCVs is a three-unit combination. Type-A vehicle consists of truck (first unit), a dolly (second unit), and a semi-trailer (third unit), while type-B vehicle comprises a tractor (first unit), a semi-trailer (second unit), and a center axle trailer (third unit). Although the configurations of the two LCVs are different, both of the vehicles can be treated as a multi-body system with three rigid bodies, which are connected one another by a revolute joint. From multi-body system modelling perspective, both LCVs share the same equations of motion. Figure 3 shows the single track model of the three-unit vehicle system.

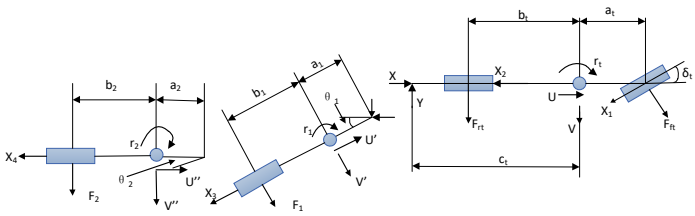

Figure 3. Schematic representation of the three-unit vehicle system.

In Figure 3, U, U' and U'' are longitudinal velocity of the first, second, and third vehicle unit, respectively, V, V' and V'' are lateral velocity of the first, second, and third vehicle unit, accordingly, r_t, r_1, and r_2 are yaw rate of the first, second, and third vehicle unit, X_1, X_2, X_3 and X_4 are tire longitudinal force of each axle, F_{ft}, F_{rt}, F_2 and F_3 are tire lateral force of each axle, I_t , I_1, and I_2 are yaw moment of inertia of the first, second, and third vehicle unit, δ_t is the leading vehicle's front axle steering angle, θ_1 and θ_2 are articulation angle between the two adjacent units, a_t, b_t, c_t, a_1, b_1, c_1, a_2, and b_2, are the length parameters of the vehicle structure, m_t, m_1, and m_2 are the total mass of the first, second, and third vehicle unit. Based on Newton's second law, the equations of motion for each vehicle unit are cast as

$$\begin{cases} m_t a_{yt} = F_{yft} + F_{yrt} - F_1 \\ I_{zt} r_t' = a_t F_{yft} - b_t F_{yrt} + c_t F_1 \\ m_i a_{yi} = F_i + F_{yi} - F_{i+1} \\ I_{zi} r_i' = a_i F_{yi} - b_i F_{yi} + c_i F_{i+1} \\ (i = 1,2) \end{cases} \quad (1)$$

Adjacent vehicle units are connected at the respective articulation joint. The velocities and accelerations at the articulation point expressed in the coordinate systems fixed with the adjacent vehicle units must be equal. This allows the trailing units' equations to be written in terms of the leading unit's body fixed coordination system. Based on the following assumptions, the equations are linearized: (1) the forward speed U is a constant; (2) δ_t, θ_1 and θ_2 are assumed to be small; (3) all products of variables are ignored; and (4) linear tire model is used.

For zero initial conditions, each articulation angle rate is correlated with the yaw rates of the respective connected vehicle units by

$$d\theta_1/dt = r_t - r_1, \quad d\theta_2/dt = r_1 - r_2 \quad (2)$$

Transforming the differential equation set (1) into a matrix form leads to

$$PX' + QX = RU \quad (3)$$

The linearized equations of motion can be written in the state-space form as:

$$X' = -P^{-1}QX + P^{-1}RU = AX + BU \quad (4)$$

$$Y = CX + DU \quad (5)$$

where the state variable vector and the output variable vector are defined as

$$X = [v_{yt} \quad r_t \quad \theta_1' \quad \theta_1 \quad \theta_2' \quad \theta_2]^T \tag{6}$$

$$Y = [v_{yt} \quad r_t \quad \theta_1' \quad \theta_1 \quad \theta_2' \quad \theta_2 \quad v_{y1} \quad r_1 \quad v_{y2} \quad r_2]^T \tag{7}$$

and matrices P, Q, and R are specified as

$$P = \begin{bmatrix} p_{11} & p_{12} & p_{13} & 0 & m_2a_2 & 0 \\ p_{21} & p_{22} & p_{23} & 0 & p_{25} & 0 \\ p_{31} & p_{32} & p_{33} & 0 & p_{35} & 0 \\ -m_2a_2 & p_{42} & p_{43} & 0 & p_{45} & 0 \\ 0 & 0 & 0 & 1 & 0 & 0 \\ 0 & 0 & 0 & 0 & 0 & 1 \end{bmatrix} \tag{8}$$

$$Q = \begin{bmatrix} q_{11} & q_{12} & q_{13} & k_1 + k_2 & \frac{L_2k_2}{v_x} & k_2 \\ q_{21} & q_{22} & q_{23} & q_{24} & q_{25} & q_{26} \\ q_{31} & q_{32} & q_{33} & q_{34} & q_{35} & q_{36} \\ -\frac{L_2k_2}{v_{xt}} & q_{42} & q_{43} & -L_2k_2 & -\frac{{L_2}^2k_2}{v_{xt}} & -L_2k_2 \\ 0 & 0 & -1 & 0 & 0 & 0 \\ 0 & 0 & 0 & 0 & -1 & 0 \end{bmatrix} \tag{9}$$

$$R = [k_{ft} \quad a_tk_{ft} \quad 0 \quad 0 \quad 0 \quad 0]^T \tag{10}$$

B. Kinematic model

In this research, a kinematic model is generated to determine the low-speed PFOT measure. The PFOT measure defines the extent that the rearmost trailer off-tracks the path of the front of the leading unit as the LCV executes a horizontal turn [10,11]. It should be noted that all vehicles need to comply with a legal requirement to be able to execute a 12.5 m radius turn. Figure 4 shows a simplified geometric relation among the vehicle units of a double-trailer AHV in a steady turn. Assuming that the turning centers of the tractor and the double trailers coincide with the point O, the two articulation angles of the double trailers need to be equal, which can make the axle midpoints D and F of the double trailers move along the track of the rear axle midpoint B of the tractor. Actually, while turning, due to the different articulation angles, the vehicle will cause swept path deviation.

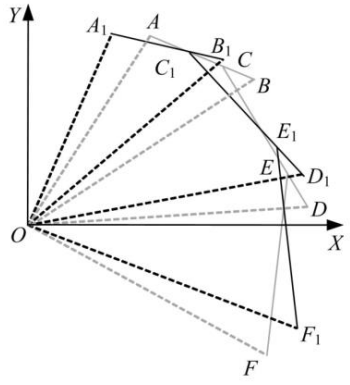

Figure 4. Simplified geometric relation among the vehicle units of an LCV.

According to the geometric relationship of the units of the LCV, the location of every point in the X-O-Y coordinate system can be obtained. For example, point A is the midpoint of the front axle of the tractor, which governs the running path of the double trailers. If point A running track is a circle of radius *R*, then $OA_1 = OA =$ R, and

$$\angle A_1OB_1 = \arccos\frac{OA_1^2 + OB_1^2 - A_1B_1^2}{2 \cdot OA_1 \cdot OB_1} \tag{11}$$

Since

$$\angle A_1Ox = \angle B_1Ox + \angle A_1OB_1 \tag{12}$$

then, the location of point *A* is determined by

$$x_1 = OA_1\cos\angle A_1OX$$
$$y_1 = OA_1\sin\angle A_1OX \tag{13}$$

In addition,

$$OB_1 = \frac{OB\sin(\angle B_1BO)}{\sin(\angle B_1OB + \angle B_1BO)} \tag{14}$$

Thus, the location of point B is determined by

$$x_2 = OB_1\cos\angle B_1OX$$
$$y_2 = OB_1\sin\angle B_1OX \tag{15}$$

Similarly, the location of point E is determined by

$$x_5 = OE_1\cos\angle E_1OX$$
$$y_5 = O\,E_1\sin\angle E_1OX \tag{16}$$

and, the location of point *F* is given by

$$x_6 = OF_1\cos\angle F_1OX$$
$$y_6 = OF_1\sin\angle F_1OX \tag{17}$$

Given the trajectories of points A and B, and those of point E and F, the low-speed PFOT measure can be calculated.

III. Simulation Results and Discussion

The vehicle parameters for the simulations were taken from the actual prototypes of LCVs [1]. The configurations of the two LCVs are shown in Figure 2. Both of them have the same total length of 25.25 m and total weight of 40 ton, while the two LCVs exhibit the difference in geometric parameters of the trailing units, i.e., dolly and trailer. The specified parameters are listed in Table 1. The simulations were conducted in Matlab based on the models generated for evaluating the high-speed lateral stability and low-speed PFOT.

A Lateral Stability

To assess the lateral stability of the LCVs, two tests are simulated: 1) step input test of steering wheel angle, and 2) sinusoid input (single cycle) test of steering wheel angle. The following subsects present and analyze the simulation results.

1) Step input test of steering wheel angle

The vehicle ran at a speed of 10 m/s in this simulation. A steering wheel angle δ_t was generated as rapidly as possible, and the angle reached the preselected value of 0.06 rad, then maintained at this value until four seconds after the measured vehicle motion variables reached a steady state.

Parameters	Type-A			Type-B		
	truck	***dolly***	***semi-trailer***	***tractor***	***semi-trailer***	***center axle trailer***
Dimension (m)	9475 *2540 *4000	4900 *2550 *1100	13600 *2550 *4000	7135 *2490 *3950	13600 *2550 *4000	7820 *2550 *4000
Mass (kg)	10000	3000	7000	9000	7000	4000
Payload (kg)	16000	-	24000	-	24000	16000
Yaw momentum of inertia （kg•m）	75697	8322	171572	20610	171572	29767
Wheelbase (mm)	4804 +1363	1328	1295 +1325	3000 +1370	8115 +1310	5440 +1800
Distance from CoG to front axle (mm)	1009	3950	4426	1714	3493	6430
Tire cornering stiffness (N/rad)	135010 477620	550360	550360	135010 477620	550360	550360

TABLE I. VEHICLE PARAMETERS VALUES FOR TYPE-A AND -B LCVS

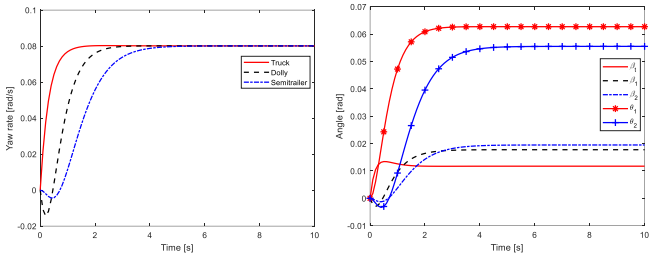

(a) Type-A (truck + dolly + semitrailer)

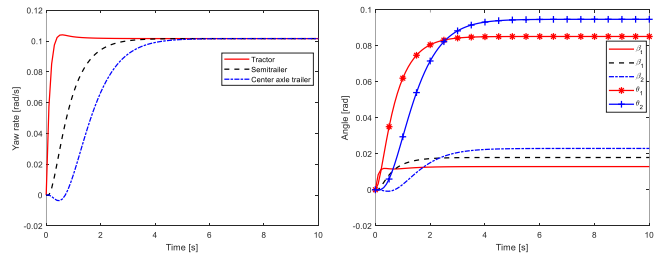

(b) Type-B (tractor + semitrailer + CAT)

Figure 5. Simulation results based on step input of steering wheel angle.

As shown in Figure 5(a), for type-A vehicle, over the step input test, the time required for the truck, dolly and semi-trailer to reach their steady state values is 1.7, 3.3 and 4.7s, respectively. The towing truck is the first to reach the stable state, followed by dolly and finally by semi-trailer. While for type-B vehicle, the time for reaching the steady state values is 1.8, 3.8, and 4.9s, respectively, and they are longer than their counterparts of type-A. The yaw rate of towing tractor experiences a small overshoot, i.e., the yaw rate of towing tractor reaches the peak value of 0.104 rad/s at the time instant of 0.6s, then decreases and reaches a stable value of 0.101rad/s at the time instant of 1.2s. Moreover, for both LCVs, the side slip angle of the rearmost unit, β_2, has the maximum value while reaching its steady state; in the case of type-A, the steady state value is 0.020 rad for the semi-trailer, while for type-B vehicle, the steady state value is 0.022 rad for the center axle trailer. The above simulation results indicate that the rearmost vehicle unit for both LCVs experiences amplified motion with respect to the leading vehicle unit. Compared with type-B LCV, type-A shows better transient dynamic responses and superior steady state behaviors.

2) Sinusoidal input (single cycle) test

To evaluate the transit dynamic behaviors of AHVs, a high-speed single lane-change maneuver with a sinusoidal steering input at a constant speed may be simulated [12,13]. In the virtual test, the vehicle was driven at the forward speed of 24.4 m/s, and a single cycle sinusoidal steering-wheel input was applied with a frequency of 0.5 Hz.

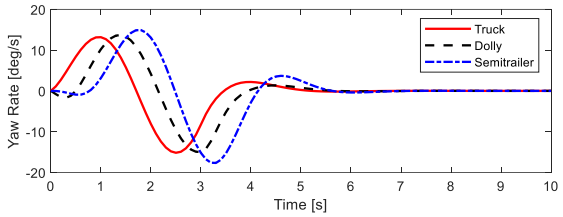

(a) Type-A (truck + dolly + semitrailer)

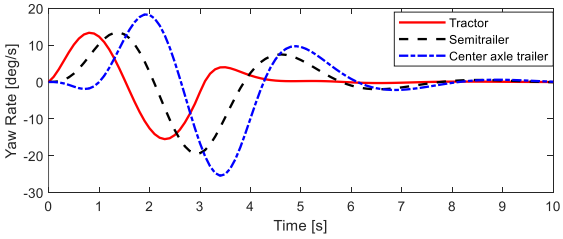

(b) Type-B (tractor + semitrailer + CAT)

Figure 6. Simulation results under the single lane-change maneuver.

Figure 6 shows the time histories of yaw rate of each unit for both type-A and -B vehicles. For both LCVs, the yaw rate of each unit shows a similar behavior, but the timing and amplitude of each curve is different. Compared with the leading unit, the trailing units show time delays, and the rearmost exhibits longer delay. The rearmost unit experiences the largest amplitude, and the amplified yaw motion of trailing units occurs. Type-A shows higher lateral stability with the yaw rate RWA of 1.13 compared with the measure of 1.36 for type-B.

B Low-speed path-following tests

To evaluate the low-speed PFOT performance of the two LCVs, the following two path-following maneuvers were simulated [14]: 1) 90-degree intersection turn, and 2) 360-

degree roundabout. Figure 7(a) schematically shows the specified 90-degree turn, which begins with a straight path, follows a curve to the right with a radius of 12.5 m, finally tracks a tangent path to resume straight stable motion. Figure 7(b) illustrates the path boundaries of the roundabout test. Over the maneuver, the testing vehicle is not allowed to violate the specified circular path with the outer and inner diameter of 25 and 10.6 m, respectively. During the testing maneuver, the PFOT measure is acquired.

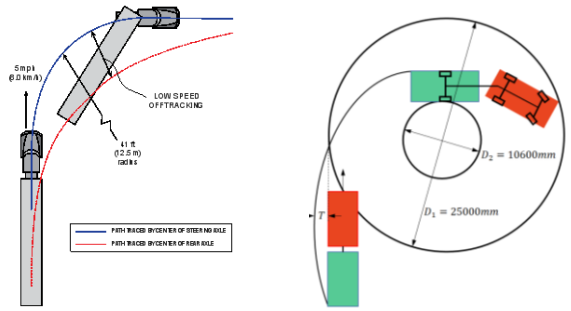

(a) (b)

Figure 7. Low-speed path-tracking maneuvers: (a) 90° turn, (b) roundabout.

Figure 8 shows the simulation results of type-A and B vehicles under the 90-degree turn. Note that in the figure, A trajectory represents the path of point A (i.e., the leading unit's front axle center as shown in Figure 4), where F trajectory denotes the path of point F (i.e., the rearmost unit's rear axle center as seen in Figure 4). For both LCVs, their A trajectories are identical, where their F trajectories are different. To distinguish the difference of their F trajectories, the blue dot curve denotes the F trajectory of type-A, while the green dot curve represents the F trajectory of type-B. It is observed that type-A exhibits poorer low-speed path-following performance with the PFOT measure of 3.5m, while type-B displays a better performance with a lower measure of 3.1m.

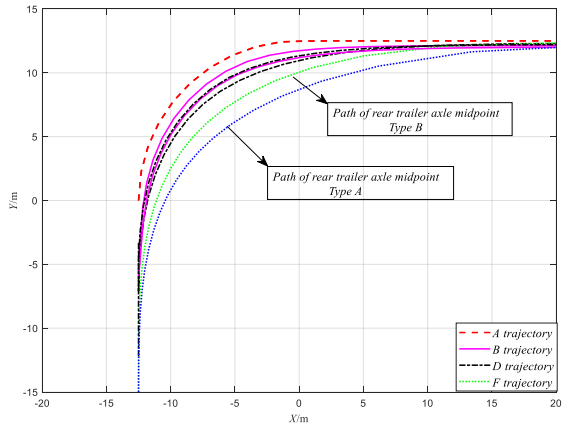

Figure 8. Simulation results of the two LCVs under the low-speed 90° turn.

It should be mentioned that for both the LCVs, due to their overall length of 25.25, it may be difficult for them to successfully execute the roundabout test without violating the path boundaries shown in Figure 7(b). To ensure the successful roundabout test, the geometric parameters of the two LCVs need to be 'optimized', and the fine-tuned values are listed in Table I. As shown in Figure 9, under the condition that the trajectories of the leading units of the two LCVs are the same, the paths of the innermost trailer tires of the two vehicles can be compared. A close observation of Figure 9 discloses that type-B shows superior PFOT performance than that of type-A.

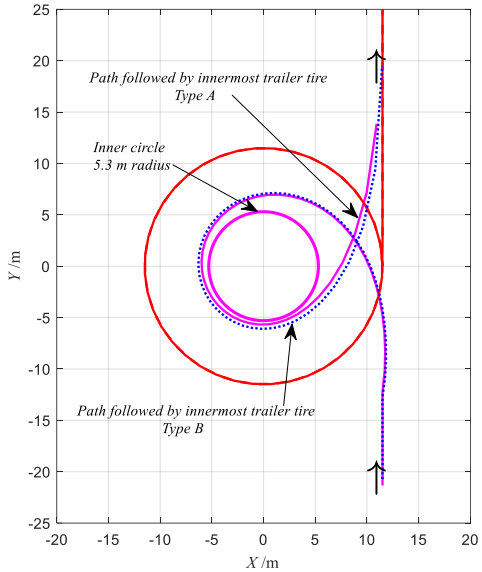

Figure 9. Simulation results of the two LCVs under roundabout test.

Based on the simulation results shown in Figures 5, 6, 8 and 9, the following points can be achieved: 1) type-A shows better high-speed lateral stability than that of type-B, and 2) type-A displays poorer low-speed PFOT performance than that of type-B. The above results are consistent with a rule-of-thumb observation pertaining to the trade-off relations between AHVs' low-speed maneuverability and high-speed stability: 'what one does to improve low-speed performance is likely to degrade high-speed performance and vice versa" [10].

C Transportation and logistics

LCVs can realize the so-called drop-and-pull operation mode switching, thereby increasing goods delivery flexibility and improving transport efficiency. In the case of type-A vehicle, for long-distance highway operations, the truck may pull the full trailer (i.e., the dolly+semi-trailer) with full payload for freight transport with high fuel-economy and low greenhouse gas emissions; for urban goods delivery, without the full trailer, the rigid truck may operate alone and negotiate urban roads and streets with high curvatures. This drop-and-pull operation mode switching is advantageous for the logistics supply chain development for intercity and urban areas in China. Thus, type-A is more suitable for the requirement. In terms of cargo capacity, there is not big difference between the two LCVs. The overall length and the maximum payload for both of the LCVs are the same, i.e., 25.25 m and 40 tons, respectively.

IV. CONCLUSIONS

To identify an effective AHV in terms of modular configuration, two LCVs are compared in directional performance, including the lateral stability and maneuverability. Based on multi-body system dynamics,

unified vehicle model for the two LCVs was generated. The main performance measures of the LCVs are acquired through simulating typical testing maneuvers. The insightful findings of the research are given as follows:

1) Type-A vehicle with the configuration of 'truck + dolly + semi-trailer' has a better lateral stability, which can meet the high-speed driving safety requirement on roads. Although the low-speed PFOT is slight worse than that of type-B vehicle with the structure of 'tractor + semitrailer + central-axle-trailer'. Alternative or advanced techniques, such as passive trailer steering [15] or active trailer steering [16], may be applied to compensate this drawback of type-A.

2) Type-B shows a poor lateral stability, but exhibits a good path-following capability. For improving the lateral stability, advanced control techniques, e.g., trailer differential braking, may be applied to ensure safe operations.

3) Type-A is more suitable for the requirements of China's freight transportation for intercity and urban areas. LCVs with modular configurations can easily realize drop-and-pull transport, thereby increasing the flexibility and goods delivery efficiency. Drop-and-pull transport is advantageous for the logistics supply chain development in China.

Therefore, type-A vehicle is recommended due to its better high-speed stability, and the advanced techniques, such as active trailer steering, may be applied to enhance the low-speed path-following performance. Type-A vehicle is featured the drop-and-pull operating mode switching, thereby being more suitable for the freight transportation and logistics of China.

REFERENCES

[1] Åkerman, I., Jonsson, R. European modular system for road freight transport- experiences and possibilities, *Trafikudvalget TRU alm*. del - Bilag 495 Offentligt, Report 2007, URL:https://www.ft.dk/samling/20061/almdel/tru/bilag/495/384322.pdf.

[2] S. Zhu, Z. Ni, A. Rahimi, and Y. He, "On dynamic stability evaluation methods for long combination vehicles," Vehicle System Dynamics, vol. 60, pp. 3999-4034, 2022.

[3] Kharrazi, S., Lidberg, M., Fredriksson, J.. A generic controller for improving lateral performance of heavy vehicle combinations. Proceedings of the Institution of Mechanical Engineers, Part D: Journal of Automobile Engineering, 2013, Vol.227, 619 - 642.

[4] Y. He, M.M. Islam, Z. Zhu, and T. Hu, "A design synthesis framework for directional perforamnce optimization of multi-trailer articulated heavy vehicles with trailer lateral dynamics control systems," *Proc IMechE Part D: J Automobile Engineering*, vol. 231(8), pp. 1096-1125, 2017.

[5] Emilio Larrodéa,Victoria Muerzab. European Modular Systems performances comparison in freight transport operations. Transportation Research Procedia 58 (2021) 165–172. doi: 10.1016/j.trpro.2021.11.023

[6] The State Council Information Office of the People's Republic of China, Sustainable Development of Transport in China [Report], December 2020, http://www.scio.gov.cn/zfbps/ndhf/42312/Document/1695302/1695302.htm

[7] Jesse Brown, Yuping He, and Haoxiang Lang, Quantifying Drivers' Driving Skills with Closed-Loop Directional Performance Measures of Articu-lated Heavy Vehicles, *Simulation Modelling Practice and Theory*, 2020, Vol.99, 102014, doi:10.1016/j.simpat.2019.102014

[8] He, Y.; Manjurul Islam, M.. An automated design method for active trailer steering systems of articulated heavy vehicles. *Transactions of the ASME*, 2012 Vol. 134, No. 4, 041002.1-041002.15, doi:10.1115/1.4006047

[9] Naser Esmaeili, Reza Kazemi. Development of the active disturbance rejection control method for increasing the stability of the long articulated vehicle[J]. *Proceedings of the Institution of Mechanical Engineers, Part D: Journal of Automobile Engineering*,2019,233(13).

[10] Fancher, P.; Winkler, C., Directional performance issues in evaluation and design of articulated heavy vehicles, *Vehicle System Dynamics*, vol. 45, No. 7–8, 607-647, 2007.

[11] Y. He, M.M. Islam, and T. Webster, "An integrated design method for articulated heavy vehicles with active trailer steering systems," *SAE Int. J. Passeng. Cars – Mech. Syst.* vol. 3(1), pp. 158-174, 2010.

[12] Q. Wang, and Y. He, "A study on single lane-change manoeuvres for determining rearward amplification of multi-trailer articulated heavy vehicles with active trailer steering systems," *Vehicle System Dynamics*, vol. 54(1), pp. 128-149, 2016.

[13] Z. Ni, S. Zhu, and Y. He, "A comparison of test manoeuvres for determining rearward amplification of articulated heavy vehicles," *Int. J. Heavy Vehicle System*, vol (27(4), pp.405-421, 2020.

[14] X. Ding, S. Mikaric, and Y. He, "Design of an active trailer-steering system for multi-trailer articulated heavy vehicles using real-time simulations," *Proc IMechE Part D: J Automobile Engineering*, vol. 227(5), pp. 643-655, 2013.

[15] B. Jujnovich, and D. Cebon, "Comparative performance of semi-trailer steering systems," Proceedings of the 7th International Symposium on Heavy VehicleWeights and Dimensions; 2002; Deft.

[16] M.M. Islam, X. Ding, and Y. He, "A closed-loop dynamic simulation-based design method for articulated heavy vehicles with active trailer steering systems," *Vehicle System Dynamics*, vol. 50(5), pp. 675-697, 2012.

Appendix

$$\begin{cases} p_{11}=m_t+m_1+m_2 \quad p_{12}=-m_1(c_t+a_1)-m_2(c_t+L_{c1}+a_2) \\ p_{13}=m_1a_1+m_2(L_{c1}+a_2) \quad p_{21}=-m_1(c_t+a_1)-m_2(c_t+L_{c1}+a_2) \\ p_{22}=I_{zt}+I_{z1}+I_{z2}+m_1a_1(c_t+a_1)-m_2(L_{c1}+a_2)(c_t+L_{c1}+a_2) \\ p_{23}=-I_{z1}-I_{z2}-m_1a_1(c_t+a_1)-m_2(L_{c1}+a_2)(c_t+L_{c1}+a_2) \\ p_{25}=-I_{z2}-m_2a_2(c_t+L_{c1}+a_2) \quad p_{31}=-m_1a_1-m_2(L_{c1}+a_2) \\ p_{32}=I_{z1}+I_{z2}+m_1a_1(c_t+a_1)+m_2(L_{c1}+a_2)(c_t+L_{c1}+a_2) \\ p_{33}=-I_{z1}-I_{z2}-m_1a_1^2-m_2(L_{c1}+a_2)^2 \quad p_{35}=-I_{z2}-m_2a_2(L_{c1}+a_2) \\ p_{42}=I_{z2}+m_2a_2(c_t+L_{c1}+a_2) \quad p_{43}=-I_{z2}-m_2a_2(L_{c1}+a_2) \\ p_{45}=-I_{z2}-m_2a_2^2 \end{cases} \tag{A.1}$$

$$\begin{cases} q_{11}=\dfrac{k_{ft}+k_{rt}+k_1+k_2}{v_{xt}} \quad q_{12}=(m_t+m_1+m_2)v_{xt}+q_{121} \\ q_{13}=\dfrac{L_1k_1+(L_{c1}+L_2)k_2}{v_{xt}} \quad q_{21}=\dfrac{a_tk_{ft}-b_tk_{rt}-(c_t+L_1)k_1-(c_t+L_{c1}+L_2)k_2}{v_{xt}} \\ q_{22}=-m_1(c_t+a_1)v_{xt}-m_2(c_t+L_{c1}+a_2)v_{xt} \\ +\dfrac{a_t^2k_{ft}+b_t^2k_{rt}+(c_t+L_1)^2k_1+(c_t+L_{c1}+L_2)^2k_2}{v_{xt}} \\ q_{23}=-\dfrac{L_1(c_t+L_1)k_1+(L_{c1}+L_2)(c_t+L_{c1}+L_2)k_2}{v_{xt}} \\ q_{24}=-(c_t+L_1)k_1-(c_t+L_{c1}+L_2)k_2 \quad q_{25}=-\dfrac{L_2(c_t+L_{c1}+L_2)k_2}{v_{xt}} \\ q_{26}=-(c_t+L_{c1}+L_2)k_2 \quad q_{31}=-\dfrac{L_1k_1+(L_{c1}+L_2)k_2}{v_{xt}} \\ q_{32}=-m_1a_1v_{xt}-m_2(L_{c1}+a_2)v_{xt} \\ +\dfrac{L_1(c_t+L_1)k_1+(L_{c1}+L_2)(c_t+L_{c1}+L_2)k_2}{v_{xt}} \\ q_{33}=-\dfrac{L_1^2k_1+(L_{c1}+L_2)^2k_2}{v_{xt}} \quad q_{34}=-L_1k_1-(L_{c1}+L_2)k_2 \\ q_{35}=-\dfrac{L_2(L_{c1}+L_2)k_2}{v_{xt}} \quad q_{36}=-(L_{c1}+L_2)k_2 \\ q_{42}=\dfrac{L_2(c+L_{c1}+L_2)k_2}{v_{xt}}-m_2a_2v_{xt} \quad q_{43}=-\dfrac{L_2(L_{c1}+L_2)k_2}{v_{xt}} \end{cases} \tag{A.2}$$